

A Photogrammetric and Theoretical Analysis of the CHIME Antenna Feed Positions

Mohamed Shaaban*

*Department of Physics and Astronomy, University of British Columbia
6224 Agricultural Road, Vancouver, British Columbia, Canada, V6T 1Z1*

(Dated: February 11, 2019)

The Canadian Hydrogen Intensity Mapping Experiment (CHIME) is a transit interferometer located at the Dominion Radio Astrophysical Observatory (DRAO) in Penticton, BC, Canada. The interferometer relies on a regular array of 1024 dual polarized antenna feeds. We will use photogrammetry techniques to produce high accuracy measurement of the feed positions relative to each other, thereby determining any irregularities in the array. The results will then be analyzed in order to (1) mechanically increase array regularity and (2) numerically correct for the arising systematic errors in sky data.

I. MOTIVATION

The most revolutionary discovery in cosmology since Hubble observed that the Universe is expanding is that this expansion is accelerating. A revelation that was awarded the 2011 Nobel Prize for its profound implications. [1]. An accelerating universe implies that either our understanding of gravity is flawed or that a mysterious pressure known as Dark Energy is driving the expansion [2]. This Dark Energy accounts for most (68.3%) of the energy in the observable universe, however its origin and physics are presently unknown [3]. As a result, the nature of Dark Energy is considered one of the greatest mysteries of modern science [4].

One of the most promising techniques to probe Dark Energy is measuring the baryon acoustic oscillation (BAO), a large scale feature of the matter distribution in the universe left over from the aftermath of the big bang (see section II A). A novel way to perform this measurement is to use fluctuations in the distribution of the most abundant element in the universe; hydrogen [5].

The Canadian Hydrogen Intensity Mapping Experiment (CHIME) is a large transit radio telescope that aims to uncover the mysteries of Dark Energy. CHIME will map the BAO providing a history of the expansion of the universe and thereby the history of Dark Energy [6]. CHIME is composed of four 100 x 20 m cylindrical reflectors with 1024 dual polarized antenna feeds positioned on the focal lines (Figure 1). The telescope is designed to operate in the frequency range 400-800 MHz encompassing the epoch when dark energy began to dominate the energy density of the Universe [7].

CHIME uses a technique known as interferometry in order to observe the sky (see section II B). CHIME's back-end operates under the assumption that the feeds form a regular lattice acting as a large interferometer array. However, in practice it is impossible to achieve

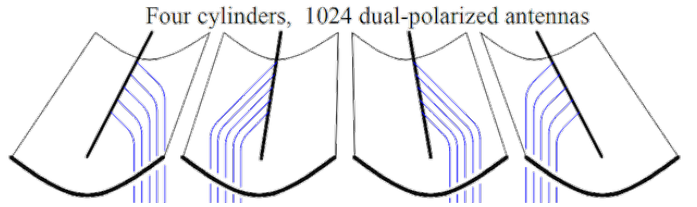


FIG. 1: This is a diagram of the CHIME instrument. CHIME is composed of four fixed cylindrical reflectors with dimensions of 100 x 20 m, where the antenna feeds are arranged along the focal lines. The location of the feeds are indicated in this diagram with the blue lines.

a perfectly regular lattice. As a result, there currently exists irregularities in the positions of the feeds. Such irregularities would induce systematic errors in the BAO measurements, and create additional challenges in the foreground removal process (removing noise from our galaxy and other near by objects).

We aim to use photogrammetry techniques to accurately determine the location of the feeds. The results will then be used to (1) mechanically move the feeds to increase the regularity of the lattice. (2) Calculate the impact the measured irregularities will have on the data in order to correct for them pre-analysis (indicated by the blue lines).

II. THEORY

In this section, we briefly elaborate on the theory behind BAO and 21cm emission. We then discuss interferometry in some detail with an emphasis on position uncertainty.

A. Baryon Acoustic Oscillations (BAO) & 21cm Cosmology

The early universe consisted of a hot and dense plasma in which baryons and electrons were too energetic to

*Electronic address: mshaaban@physics.ubc.ca

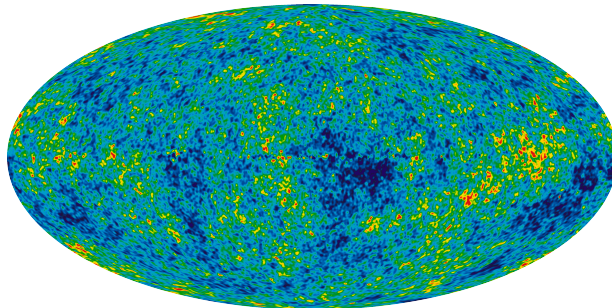


FIG. 2: Temperature map of the Cosmic Microwave Background based on WMAP data. The change in colour represents the fluctuations in temperature distribution and thereby fluctuations in the matter density distribution [8].

combine, resulting in a charged plasma where photons were constantly scattering off matter unable to travel far [6]. This interaction results in a pressure acting in the opposite direction of gravity [9]. This pressure drives oscillation in the density of matter in a manner similar to that of sound waves in air, i.e. given an overdense region in the plasma, baryons and photons will propagate outwards in a mechanism similar to that of a spherical sound wave [9, 10]. These oscillations are what we refer to as Baryon Acoustic Oscillations (BAO).

Around 380,000 years after the big bang the universe had cooled enough to allow electrons and protons to combine forming neutral hydrogen. At that moment the universe became transparent as photons became free to radiate away unimpeded, creating the Cosmic Microwave Background (CMB) (see Figure 2) and putting an end to the radiation pressure that was driving the BAO. As a result the matter distribution froze with only gravity guiding any subsequent evolution in density [6]. The distance traveled by the sound wave up until this point is about 150 Mpc ($4.6 \times 10^{24} m$) [9]. On this scale the expansion of the universe becomes the dominating factor in the evolution of the matter distribution. This means that BAO provide a length scale that can be used to probe the expansion history of the universe [9, 11]. Since dark energy is the entity responsible for the accelerating expansion of the universe, probing the expansions history is the best cosmological probe for dark energy [11].

Most of the ordinary matter in the universe is composed of neutral hydrogen, therefore mapping the hydrogen intensity of the universe is a promising method for accurately measuring BAO [12]. One can map the hydrogen in the universe by looking for 21 cm hyperfine transition emission from neutral hydrogen. This is a transition between the two lowest energy levels in hydrogen arising as a result of spin-spin coupling between the proton and the electron [13]. The hyperfine energy gap is $5.88 \times 10^{-6} eV$, therefore a photon emitted through this

transition has a wavelength of $\approx 21cm$ (hence the name) [13]. This wavelength falls in the radio range, which is advantageous for surveys as they can penetrate cosmic clouds and reach us smoothly, additionally it is isolated in the astronomical radio spectrum making it practical for obtaining the redshift of the observed source [14].

B. Interferometry

Interferometry is the method of superimposing waves in order to extract information from their interference. The basic interferometer is composed of two antenna whose outputs are correlated. This method and its applications to astronomy is best illustrated by studying the simplest example of a radio interferometer, the two-element quasi-monochromatic interferometer. This simple example is of crucial importance as even the most elaborate interferometers (e.g. CHIME) with $N >> 2$ antennas can be treated as $N(N - 1)/2$ independent interferometer pairs [15]. Therefore, we study this example in detail highlighting its relevance to the project (i.e. the importance of knowing the feed positions with a high accuracy).

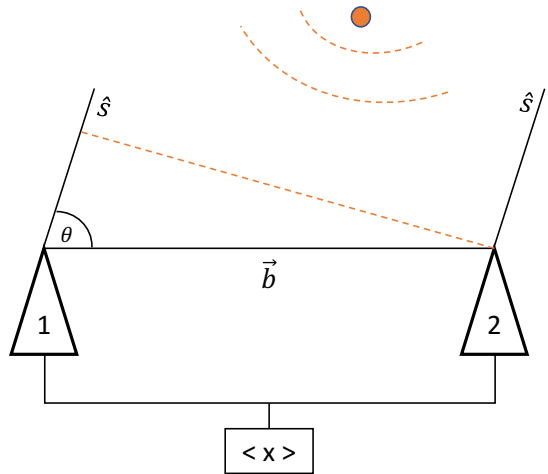


FIG. 3: This is a diagram of a two-element interferometer. The two triangles labeled 1 and 2 represent two antenna separated by a baseline vector \vec{b} . The straight orange line represents the wavefront coming from a source in the \hat{s} direction, feeds 1 and 2 are receiving the same signal with a phase offset due to the path difference seen in the diagram (the path to feed 1 is $\vec{b} \cdot \hat{s}$ longer than the path to feed 2) The $\langle x \rangle$ component of the diagram represents the correlator, the component responsible for combining the signal from the two feeds.

1. Two-Element Quasi-Monochromatic Interferometer (Point Source)

As the name suggests this interferometer uses two antenna feeds to observe a very narrow frequency range

centered at $\nu = \omega/(2\pi)$ (see Figure 3). Consider a point source stationary in the sky (relative to our reference frame), then the feeds output voltages are time dependant and are represented by $V_i = V \cos(\omega t)$. These voltages are sent to the correlator where they are amplified, multiplied and averaged.

The diagram (Figure 3) clearly indicates a difference between the paths traveled by the wave-front to reach the two antenna, the path to feed 1 is $\vec{b} \cdot \hat{s}$ longer than the path to feed 2. Were \vec{b} is the baseline separation vector between the two feeds and \hat{s} is the direction from which the wave-front is approaching. As a result we have an offset in the phase of feed 1 by

$$\tau = \frac{\vec{b} \cdot \hat{s}}{c} \quad (1)$$

where c is the speed of light. Therefore, at a given time t the output voltages of the feeds are given by

$$V_1 = V \cos(\omega(t - \tau)) \quad (2a)$$

$$V_2 = V \cos(\omega t) \quad (2b)$$

these voltages are multiplied in the correlator yielding $V_1 V_2 = V^2 \cos(\omega(t - \tau)) \cos(\omega t) = (V^2/2)(\cos(\omega\tau) + \cos(2\omega t - \omega\tau))$ the correlator then takes a time average long enough to remove the $\cos(2\omega t - \omega\tau)$ term. Leaving us with the final correlator response as

$$R_c = \langle V_1 V_2 \rangle = \left(\frac{V^2}{2} \right) \cos(\omega\tau) \quad (3)$$

This example highlights the importance of knowing the value of \vec{b} to a high accuracy, uncertainty in the feed positions would result in calculating a false \hat{s} from a given output τ , i.e. our telescope is not "pointing" where we think it is.

2. Two-Element Quasi-Monochromatic Interferometer (Extended Source)

Since in general a source is not limited to behaving as a point source, we briefly generalize the previous calculation to account for extended sources.

The idea is to treat an extended source as a sum of independent point sources, with $I_\nu(\hat{s})$ representing the sky brightness distribution near the frequency ν . Building on the previous calculation we have the correlator response as

$$\begin{aligned} R_c &= \int I_\nu(\hat{s}) \cos(\omega \vec{b} \cdot \hat{s}/c) d\Omega \\ &= \int I_\nu(\hat{s}) \cos(2\pi \vec{b} \cdot \hat{s}/\lambda) d\Omega \end{aligned} \quad (4)$$

were Ω is the solid angle. However, this response is clearly only sensitive to the even component of the brightness distribution, i.e. we need to add in the odd component. This can be done by including a second correlator output with a 90 degree phase delay resulting in

$$R_s = \int I_\nu(\hat{s}) \sin(2\pi \vec{b} \cdot \hat{s}/\lambda) d\Omega \quad (5)$$

We now combine the two responses to achieve the desired result. We define the visibility $\mathcal{V} = R_c + iR_s$ giving us the final response to an extended source as

$$\mathcal{V} = \int I_\nu(\hat{s}) e^{-i2\pi \vec{b} \cdot \hat{s}/\lambda} d\Omega \quad (6)$$

Again we note the explicit dependance on \vec{b} highlighting the importance of knowing the value to a high accuracy. For completeness we also point out that this result can be further generalized for a finite frequency range. This can be done by integrating over ν in the desired range prior to integrating over Ω .

3. Far-Field Approximation

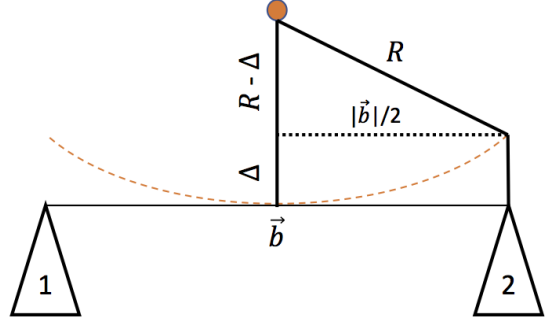


FIG. 4: This diagram shows the same interferometer as FIG3, the orange line represents the spherical wave front upon arrival at the feeds. The parameter Δ parameterizes the deviation from a planar wave and R represents the distance between the wave and the source.

It is clear that the above calculations rely on the underlying assumption that the wave-front is a straight line, i.e. the waves are planar. In this subsection we perform a quick calculation to verify that this assumption is justified. Consider the set up in Figure 4, by Pythagoras theorem we have

$$R^2 = (R - \Delta)^2 + \left(\frac{|\vec{b}|}{2} \right)^2 \implies R = \frac{\Delta}{2} + \frac{|\vec{b}|^2}{8\Delta} \quad (7)$$

therefore in the limit $\Delta \ll |\vec{b}|$, we have $\Delta/2 \ll |\vec{b}|^2/(8\Delta)$ and as a result

$$R \approx \frac{|\vec{b}|^2}{8\Delta} \quad (8)$$

It is clear that as R goes to infinity Δ goes to 0, i.e. for sources far away we can treat an incoming spherical wave as planar. In practice we require the source to be at a distance such that $\Delta \ll \lambda$, a somewhat arbitrary convention is to require $\Delta < \lambda/16$ therefore requiring the source to be further than $2|\vec{b}|^2/\lambda$. For CHIME that distance is on the order of 5km, meaning our approximation holds for astronomical sources.

III. DETAILS ON PROPOSED EXPERIMENT

The experiment will be conducted through four phases, with the second and third phase occurring simultaneously and accounting for the bulk of the project.

A. Software Testing Phase

The first phase of the experiment will be dedicated to finding photogrammetry software that is compatible with our goals. I will research the available photogrammetry software and will make a choice based on its features, user friendliness, export capabilities and cost. At the time of writing this proposal Agisoft Photoscan is the lead candidate.

After the software is chosen a mock experiment will be set up in order to simultaneously familiarize myself with the software and assess its accuracy. The mock experiment will simply involve setting up markers with a known separation, photographing them and analyzing the photos using the software.

B. Photogrammetric Analysis Phase

This phase will revolve around performing the photogrammetric analysis on drone captured pictures of the CHIME feeds. This phase is partitioned into three main tasks.

The first and perhaps simplest task is to use the data to produce a 3D model of the focal line. This is a process that is almost entirely automatic through the software. The second task is to utilize the fact that the feeds are a distinct color from their surroundings in order to automate their tagging. This task is crucial as manually tagging all 1024 feeds would limit our ability to reanalyze the data. The third and final task is to extract the feed position data from the 3D model. The data needs to be exported and formatted in a manner that is useful and useable by the collaboration.

Realistically this phase will be repeated several times, each 3D model will potentially highlight weaknesses in our photo set, enabling us to go back and capture additional photos to add onto the model with each iteration.

C. Theoretical Calculations Phase

The focus of this phase is to theoretically understand how perturbations in the feed positions will impact CHIME data. Due to the complexity of this task we will perform a series of analytic and numerical calculations in a series of steps leading up to the main calculation.

The first step is to simply calculate the primary beam (telescope's sky sensitivity) of a parabolic reflector. This is to further familiarize myself with the mathematics behind the problems at hand. Once this calculation is completed I will move on to the simplest version of the original problem, I will calculate the effects of a perturbation in the feed position on a 2-dish interferometer. At this point we will be ready to begin performing CHIME feed calculations, the first step will be to consider the effects of perturbations along the focal line (North-South and vertical axis), i.e assuming that the position along the East-West axis is perfect and unperturbed. After the effects of these perturbations are well understood we will begin to incorporate East-West axis perturbations into our calculations, thereby achieving the desired understanding. Finally, the calculations will be combined with simulations to predict the effect the position uncertainty will have on CHIME BAO maps and foreground removal efforts.

D. Result Analysis Phase

The final phase is to combine our photogrammetry data with our theoretical calculations in order to understand how the measured perturbations will propagate into CHIME data. We then use those results to design a solution, we intend to use a combination of (1) mechanically adjusting the feeds to increase regularity of the lattice and (2) accounting for the errors numerically through back-end calculations.

IV. RESOURCES LIST

For this project I will need the following resources:

- A computer with at least 12GB of RAM
- Picture capable drone and an HD camera
- A means to perform numerical analysis (Python)

- High accuracy 3D model producing photogrammetry software

V. PLANNED SCHEDULE

- **September:** (1) Investigate and compare available photogrammetry software and plan a strategy accordingly. (2) Analyze a proposal written by my supervisors for learning purposes. (3) Acquire drone pictures of the CHIME feeds.
- **October:** (1) Solve simple photogrammetry problems by hand to further familiarize myself with the theory behind the process. (2) Design and conduct a mock experiment that will be used to assess the accuracy of the available photogrammetry software. (3) Perform a soft analysis on the drone data for troubleshooting purposes.
- **November:** (1) If necessary acquire and analyse

new drone data. (2) Complete writing the proposal and accompanying talk.

- **December-January:** (1) Write the general science and introduction chapters of the thesis. (2) Begin designing a strategy to fix (regularize) the positions of the feeds. (3) Further familiarize myself with the theory and mathematics behind BAO and CHIME data.
- **February:** Perform a mathematical analysis of how the results (positions of feeds) will impact our BAO and foreground data, i.e. how lattice regularity impacts data accuracy.
- **March:** (1) Implement the strategy designed for regularizing the lattice. (2) Complete the first draft of the thesis.

- [1] *The nobel prize in physics 2011 - advanced information.* nobelprize.org. (2014).
- [2] P. J. E. Peebles and B. Ratra, Rev. Mod. Phys. **75**, 559 (2003), astro-ph/0207347.
- [3] P. A. R. Ade et al. (Planck), Astron. Astrophys. **571**, A1 (2014), 1303.5062.
- [4] K. Bandura, G. E. Addison, M. Amiri, J. R. Bond, D. Campbell-Wilson, L. Connor, J.-F. Cliche, G. Davis, M. Deng, N. Denman, et al., in *Ground-based and Airborne Telescopes V* (2014), vol. 9145, p. 914522, 1406.2288.
- [5] A. Loeb and S. Wyithe, Phys. Rev. Lett. **100**, 161301 (2008), 0801.1677.
- [6] J. B. Peterson, R. Aleksan, R. Ansari, K. Bandura, D. Bond, J. Bunton, K. Carlson, T.-C. Chang, F. DeJongh, M. Dobbs, et al., in *astro2010: The Astronomy and Astrophysics Decadal Survey* (2009), vol. 2010 of *ArXiv Astrophysics e-prints*, 0902.3091.
- [7] L. B. Newburgh et al., Proc. SPIE Int. Soc. Opt. Eng. **9145**, 4V (2014), 1406.2267.
- [8] G. Hinshaw et al. (WMAP), Astrophys. J. Suppl. **180**, 225 (2009), 0803.0732.
- [9] D. J. Eisenstein et al. (SDSS), Astrophys. J. **633**, 560 (2005), astro-ph/0501171.
- [10] D. J. Eisenstein, *Measuring cosmic distances with the baryon acoustic oscillations*, University of Chicago Lecture (2008).
- [11] H.-J. Seo and D. J. Eisenstein, Astrophys. J. **598**, 720 (2003), astro-ph/0307460.
- [12] T.-C. Chang, U.-L. Pen, J. B. Peterson, and P. McDonald, Phys. Rev. Lett. **100**, 091303 (2008), 0709.3672.
- [13] D. Griffiths, *Introduction to Quantum Mechanics* (Cambridge University Press, 2016), ISBN 9781107179868, URL <https://books.google.ca/books?id=0h-nDAAAQBAJ>.
- [14] J. R. Pritchard and A. Loeb, Reports on Progress in Physics **75**, 086901 (2012), URL <http://stacks.iop.org/0034-4885/75/i=8/a=086901>.
- [15] J. J. Condon and S. M. Ransom, *Essential radio astronomy*, National Radio Astronomy Observatory (2010), URL <http://www.cv.nrao.edu/course/astr534/ERA.shtml>.